PHILOSOPHICAL TRANSACTIONS OF THE ROYAL SOCIETY B BIOLOGICAL SCIENCES

The Origin of Neuronal Polarization: A Model of Axon Formation

David C. Samuels, H. G. E. Hentschel and Alan Fine

Phil. Trans. R. Soc. Lond. B 1996 **351**, 1147-1156
doi: 10.1098/rstb.1996.0099

The origin of neuronal polarization: a model of axon formation

DAVID C. SAMUELS[1], H. G. E. HENTSCHEL[1] AND ALAN FINE[2]*

[1] *Department of Physics, Emory University, Atlanta, Georgia 30322, U.S.A.*
[2] *Department of Physiology and Biophysics, Faculty of Medicine, Dalhousie University, Halifax, Nova Scotia, Canada B3H 4H7*

SUMMARY

During development, most neurons become polarized when one neurite, generally the longest, becomes the axon and the other neurites become dendrites. The physical mechanism responsible for such length-related differentiation has not been established. Here, we present a model of neuronal polarization based upon the existence of a 'determinant chemical' whose concentration at the neurite tips influences the growth rate of the neurite. Over an extended parameter range, the equations describing the formation, transport, and consumption of this chemical and the resulting neurite growth undergo a winner-take-all instability, yielding rapid growth of one neurite (the axon) and diminished growth of all others. The behaviour of this model agrees well with the results of axotomy experiments and experiments in which growth-modulating substances are applied to individual growth cones. Possible candidates for the determinant chemical are discussed, and further experiments are proposed to test the model.

1. INTRODUCTION

Neural cells grown in culture commonly show a simple and repeatable growth pattern leading to the development of two different types of extensions: axons and dendrites. Initially, the cell projects many broad, short lamellepodia. This has been referred to by Dotti *et al.* (1988) as stage 1 of outgrowth. These lamellepodia subsequently condense into a number of small neurites, of approximately equal lengths, which undergo a period of growth and contraction (stage 2). Eventually one of the neurites rapidly increases its growth rate and acquires axonal characteristics (stage 3) while the growth rates of the other neurites are profoundly reduced. The onset of rapid growth in the presumptive axon is the first known sign of neuronal polarization, and is followed by the segregation of certain cell constituents to the axonal or somatodendritic compartments (Craig & Banker 1994). After several more days of development, the remaining neurites begin to grow again, and acquire dendritic characteristics (stage 4).

Axotomy experiments have shown that all neurites have the potential to develop into the axon (Dotti & Banker 1987; Goslin & Banker 1989). When the axon is cut during developmental stage 3, the axotomized neuron regenerates an axon, sometimes from the stump of the original axon but more often from one of the remaining minor neurites. The origin of the new axon is seemingly determined primarily by the length of the neurites, with the longest most often becoming the axon (Goslin & Banker 1989). Apparently, identical growth processes occur in every neurite, and an instability occurs which accelerates the growth rate of a single neurite, favouring the longest and inhibiting growth of all the others. How this occurs is not known. Our aim in this study has been to identify and model the mechanisms that may lead to this growth instability, and thus to neuronal polarization.

2. THE MODEL

We consider the formation, motion and consumption of a single chemical that determines the rate of growth of the neurites. Of course many substances such as cytoskeletal proteins, membrane proteins, cytoplasmic enzymes and second messengers are required for neurite growth (Matus 1988; Skene 1989; Craig & Banker 1994; Schoenfeld & Obar 1994), so the determinant chemical in this model should be interpreted as the rate-limiting substance among all of those necessary for early neurite growth. The identity of this determinant chemical is not known; we shall return to this problem later.

Following the suggestion of Goslin & Banker (1989), we hypothesize that the determinant chemical is produced in the neuronal soma and transported to the tips of the growing neurites, where it is consumed in the growth process. Depending on the identity of the determinant chemical, this consumption may be viewed as the polymerization of cytoskeletal monomers, the addition of microtubule-associated proteins (MAPS) to microtubules, the consumption of energy or metabolites in cytoskeleton assembly, or the addition of new membrane. These processes are believed to occur primarily at the distal ends of growing neurites (Letourneau & Ressler 1984; Bramburg *et al.* 1986; Gordon-Weeks 1991; Mansfield *et al.* 1991; Craig *et al.* 1995).

* To whom correspondence should be addressed.

Phil. Trans. R. Soc. Lond. B (1996) **351**, 1147–1156
Printed in Great Britain

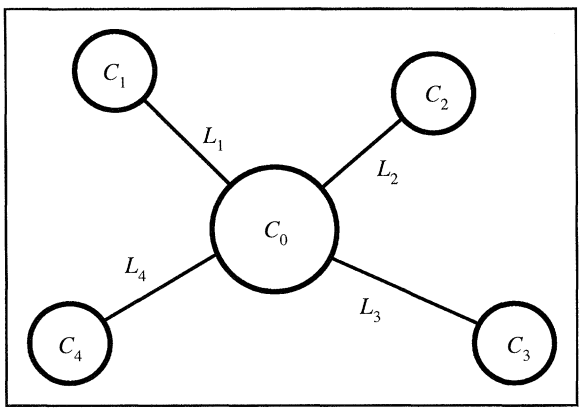

Figure 1. A schematic diagram of the simulation for a neuron with four neurites. The simulation variables are the determinant chemical concentrations in the soma (C_0) and in the tips of each neurite (C_1–C_4) and the lengths of each neurite (L_1–L_4).

The variables we examine are the concentration C_0 of the determinant chemical within the soma, the concentrations C_1 to C_N at the N neurite tips, and the neurite lengths L_1 to L_N. Figure 1 shows a schematic of these variables and their relation to the neuron morphology. The development of the concentration in the soma is given by

$$dC_0/dt = [S - \sum_{i=1}^{N} T_i]/V_{soma}, \quad (1)$$

where S is the rate of production of the determinant chemical by the cell, the i subscript labels each of the N neurites, T_i is the net transfer rate of the chemical from the soma to the neurite tip, and V_{soma} is the volume of the soma. For these simulations we will consider the production rate S to be constant. In reality, the value of this parameter is likely to change with time as the cell enters different stages of development, and it may also be dependent on C_0 so that the production decreases when the soma concentration becomes too high.

The net transfer of the determinant chemical will result from two processes, diffusion and anterograde transport (more precisely, the net result of combined retrograde and anterograde transport). These two processes will tend to counteract each other, because anterograde transport acts to concentrate material at the neurite tip whereas diffusion acts to equilibrate concentrations at the tip and soma. If a unique axon is to form, the net transfer rate must increase for the axon – in order to supply adequate determinant chemical – at the expense of the other neurites. Diffusion becomes less effective with increased neurite length, but the requisite instability only emerges if anterograde transport increases with either the length or growth rate of the neurite (see below). It is difficult to imagine how neurite length *per se* could affect the transfer rate, but an effect due to the growth rate is plausible. The transfer rate is a product of two factors: the speed of transport along the neurite and the rate at which substances enter the transport process from the soma. Then if, for example, neurite outgrowth results from traction exerted by the growing tip (Lamoureux *et al.* 1989), an increased growth rate would pull more cytosol – and thus more of the determinant chemical – into the neurite's proximal end, with access to the transport mechanism. With such a picture in mind, we model the anterograde transport as proportional to the growth rate of the neurite. The net transfer rate from the soma to the neurite tip is then

$$T_i = DA(C_0 - C_i)/L_i + F(dL_i/dt)C_0 + I_iC_0, \quad (2)$$

where D is the diffusion constant of the determinant chemical, A is the cross-sectional area of the neurite, F is a growth-dependent transport parameter and I_i is a transport parameter independent of growth (because transport may also occur in the absence of growth, for example in the mature cell; in the simulations described below, this term is always set to 0).

Because all neurites have the potential to form the axon (Dotti & Banker 1987), we model all the neurites identically. The development of the chemical concentrations C_i and the neurite lengths L_i are given by

$$dC_i/dt = [T_i - G(dL_i/dt)]/V_{tip}, \quad (3)$$

$$dL_i/dt = \alpha C_i, \quad (4)$$

where G and α are growth parameters and V_{tip} is the volume of the neurite tip where the growth processes occur. The term $G(dL_i/dt)$ represents the consumption of the determinant chemical by the growth process at a rate proportional to the growth rate. For simplicity, the growth rate of the neurite is assumed to be proportional to the local concentration of the determinate chemical C_i. More complex models for this growth rate could be used, as long as the growth rate rises with increasing concentration over some concentration range. It should be noted that equation (4) limits this model to positive velocities. Thus, the oscillations between growth and retraction that are observed in real neurites will not be seen in this model.

To reduce the number of parameters in equations (1–4) we convert them to a non-dimensional form. To do this we must choose scales for the concentration, time, and length. We choose the scales

$$C_{scale} = S/\alpha G, \quad (5a)$$

$$t_{scale} = V_{soma}/\alpha G, \quad (5b)$$

$$L_{scale} = V_{soma}\, S/\alpha G^2. \quad (5c)$$

An extreme solution of equations (1–4) is when the entire source is consumed by a single neurite, a situation that closely resembles our expectations for the growth of a single axon. In that case we have $S = G\alpha C_i$ (production equals consumption by neurite i) which we may write as $C_i = S/\alpha G$. With this as the choice for C_{scale} we can expect the non-dimensionalized concentration in any axon to be near 1. The time scale was chosen so that the non-dimensionalized source term of equation (1) would be unity. The length scale was chosen to simplify the rate of growth in equation (4). The equations in non-dimensional form are

$$d\tilde{C}_0/d\tilde{t} = 1 - \sum_{i=1}^{N} [\chi_1(\tilde{C}_0 - \tilde{C}_i)/\tilde{L}_i + \chi_2(d\tilde{L}_i/d\tilde{t})\tilde{C}_0] \quad (6a)$$

$$d\tilde{C}_i/d\tilde{t} = \chi_3[\chi_1(\tilde{C}_0 - \tilde{C}_i)/\tilde{L}_i + \chi_2(d\tilde{L}_i/d\tilde{t})\tilde{C}_0 - (d\tilde{L}_i/d\tilde{t})] \quad (6b)$$

$$d\tilde{L}_i/d\tilde{t} = \tilde{C}_i \quad (6c)$$

PHILOSOPHICAL TRANSACTIONS OF THE ROYAL SOCIETY B BIOLOGICAL SCIENCES

where a tilde marks a non-dimensionalized quantity and we define the parameters

$$\chi_1 = DAG/SV_{soma} \quad (7a)$$

$$\chi_2 = FS/\alpha G^2 \quad (7b)$$

$$\chi_3 = V_{soma}/V_{tip}. \quad (7c)$$

The nine parameters of equations (1–4) are now reduced to four (χ_1, χ_2, χ_3, N). The parameters χ_3 and N are simple geometric parameters. All of the important biological parameters have been subsumed into χ_1 and χ_2. The values of χ_1 and χ_2 for a real neuron cannot be determined until the identity of the determinant chemical is known. Nevertheless, we have observed that much of the behaviour of the solutions to equations (6) is not strongly dependent on the exact values of χ_1 and χ_2 as long as the parameters are not near their critical values for axon development.

Equations (6) are solved by a Runge–Kutta–Fehlberg method (Cheney & Kincaid 1980). Typical initial conditions are that the initial concentrations are set to zero and the initial neurite lengths are set to small random values ($\tilde{L}_i(\tilde{t}=0) < 10^{-2}$), where 'small' is defined relative to the typical length attained by the neurites that do not form the axon.

3. AXON DEVELOPMENT

Within a certain parameter range, the numerical solutions of equations (6) show an instability leading to the formation of $N-1$ very slowly growing neurites and a single quickly growing neurite which we identify as the axon. Figure 2 shows the development of the determinant chemical concentrations and neurite lengths for a typical simulation. In figure 2(*a*) we can see the rapid and continuous growth of the axon while the other neurites remain short ($\tilde{L} \simeq 0.3$). The concentration development (figure 2*b*) shows more detail. Our model (equation 6*c*) specifies that each neurite's growth rate is proportional to the determinant chemical concentration at its tip; thus this plot also describes the development of the neurite growth rates. Initially, the concentrations in the soma (dashed line) and all the neurites (solid lines) rise together. At this stage the neurites are very short and diffusion is sufficient to keep the concentrations equal. As the concentrations within the neurites increase, the soma concentration begins to fall owing to the increase in the transfer term (equation (2)) from soma to neurites. During this stage the concentrations within the neurites diverge, as one by one the neurite concentrations begin to fall. Eventually, only a single neurite is left with a high concentration. The concentration of this neurite then increases very rapidly and levels out at a value slightly less than one, while the concentrations of the other neurites decrease and level out at a very low value. This progression is stereotypical of axon development in these simulations and corresponds to neuronal developmental stages 2 and 3 as defined by Dotti *et al.* (1988). It is helpful to convert the non-dimensional times and lengths of figure 2*a* into real units to check the plausibility of the results. With typical values for the time of axon formation (20 h) and average axon growth rate (5 μm h^{-1}) taken from Dotti *et al.* (1988), the resulting length scale for figure 2*a* is 100 μm. This is only an approximate value, but it is in reasonable agreement with observations.

The simulation presented in figure 2 began with all concentrations equal to zero and a range of random neurite lengths ($\tilde{L}_1 = 0.0070$, $\tilde{L}_2 = 0.0035$, $\tilde{L}_3 = 0.0019$, and $\tilde{L}_4 = 0.0085$). The length ranking of the neurites was preserved during development, with the longest (neurite 4) becoming the axon. Note that neurite 1 had an initial length only slightly less than neurite 4, and it was also the neurite in figure 2(*b*) whose concentration continued to increase for the longest time before dropping to the final low level.

Because this simulation began with equal concentrations and random initial lengths, the possibility has to be considered that these initial conditions favour the determination of the axon based on length differences and thus obscure a possible determining role of concentration differences. To test this, we ran a series

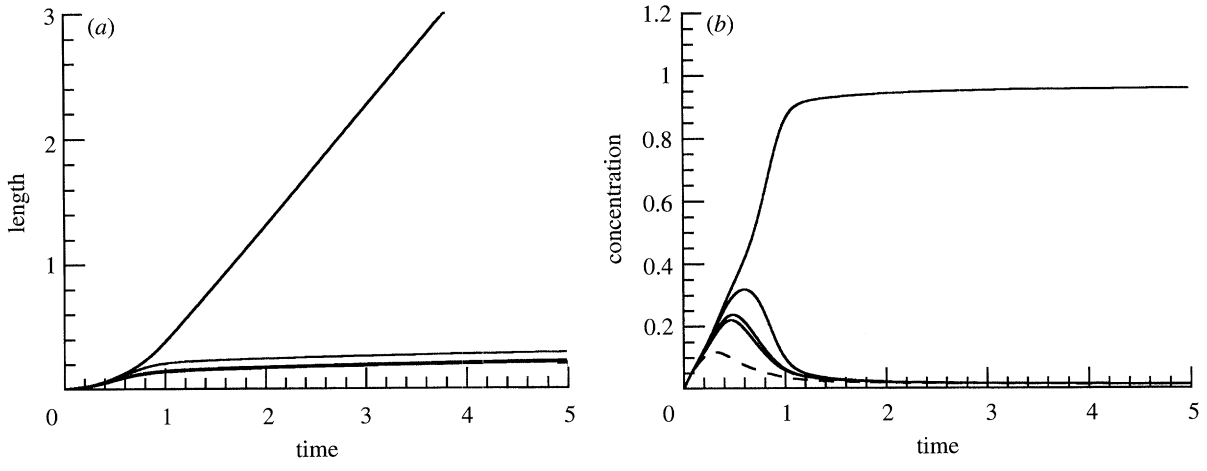

Figure 2. Typical simulation results for a cell with four neurites. Length of the neurites (*a*) and concentration of determinant chemical at their tips and in the soma (dashed line) (*b*) are plotted against time. (The heavy lowest line in (*a*) shows the growth of the two smallest neurites superimposed.) All values are dimensionless. The simulation parameters are $\chi_1 = 1$, $\chi_2 = 100$, $\chi_3 = 10$, and $N = 4$.

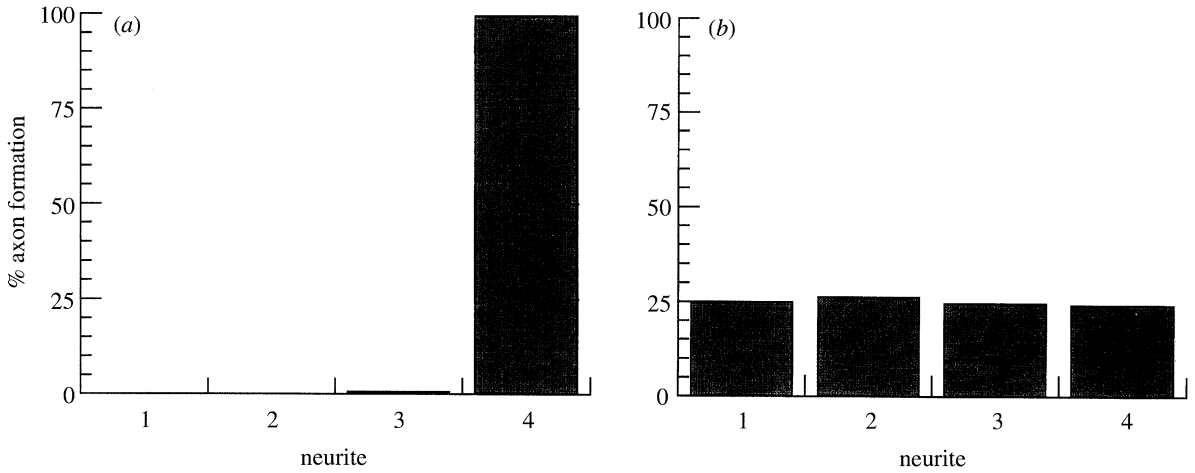

Figure 3. Correlation of the probability of axon formation with the initial conditions of the simulation. (*a*) Neurites ordered by initial length from shortest to longest. (*b*) Neurites ordered by initial concentration from lowest to highest.

of 1000 simulation runs, all with identical parameters ($\chi_1 = 1$, $\chi_2 = 100$, $\chi_3 = 10$ and $N = 4$), but with random initial conditions. The initial lengths were chosen in the range $0 < \tilde{L}_{initial} < 0.01$ and the initial concentrations were in the range $0 < \tilde{C}_{initial} < 0.1$. The neurites in each run were ranked from 1 to 4 in order of increasing initial length, and also ranked in order of increasing initial concentration. The identity of the neurite that developed into the axon was recorded for each run and these data were analysed for correlations between the probability of axon formation and the initial concentration and length rankings of the neurites (see figure 3). The correlation is striking. In 994 out of 1000 runs the initially longest neurite developed into the axon. In the remaining 6 runs the initially next-to-longest neurite became the axon. In contrast, when ranked by initial concentration the probabilities of axon formation were all within 2 % of 25 %, the value expected for no correlation. Clearly it is length perturbations that strongly influence the instability to axon formation in these equations, in agreement with the observations of Goslin & Banker (1989).

For simplicity, we have confined the perturbations in our simulations to the initial conditions. In reality, perturbations continue throughout the development of the cell. That should not change our assertion that the choice of axon is primarily dependent upon length perturbations: in tests where length and concentration perturbations were made during axon formation (at times less than $\tilde{t} = 0.5$ in figure 2) we found that concentration perturbations damped out quickly whereas length perturbations affected the choice of axon. This was surprising, considering that concentration seemed to be the critical variable in the equations. Both concentration and length, however, appear in the transport term T_i, which forms the feedback loop of the equations, and the specific contributions of these variables to the instability remains to be determined.

This model predicts that even small differences in initial neurite lengths will almost invariably lead to the longer neurite forming the axon. The model, however, does not include the quasi-random growth spurts and retractions observed during the growth of neurites in culture (Dotti *et al.* 1988); furthermore, factors that we have taken to be constant or smoothly varying, such as the determinant chemical production S and the net transport rate T_i, are likely in reality to be noisy. Such randomness would be expected to make axonal specification far less deterministic than it is in the present model.

4. INSTABILITY LEADING TO AXON FORMATION

Not all values of the parameters lead to the axon formation described above. A stability map for equations (6) may be constructed as a function of the four parameters χ_1, χ_2, χ_3, and N. To construct a useful two-dimensional map we held the geometric parameters constant at reasonable values ($\chi_3 = 10$ and $N = 4$) and concentrated on the stability as a function of the biological parameters χ_1 and χ_2. The resulting stability map is given in figure 4. We have also found that the position of the instability line varies slightly with the

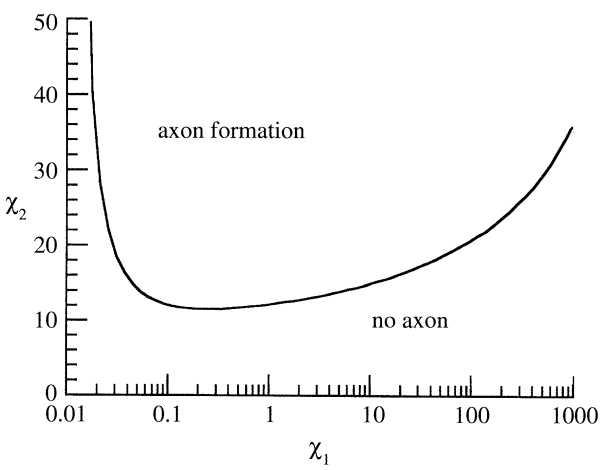

Figure 4. Stability map for the growth of axons. The map shown is for the values $N = 4$, $\chi_3 = 10$, and an initial length difference of 10^{-2}. The position of the curve depends on these parameters, but the shape of the curve does not.

PHILOSOPHICAL TRANSACTIONS OF THE ROYAL SOCIETY B BIOLOGICAL SCIENCES

magnitude of the initial length variation. In the stability map shown here we have used an initial length variation of $\delta\tilde{L}_i = 10^{-2}$. Larger variations in the initial lengths increase the size of the axon-formation region. Although the exact position of this instability line does depend on the values of χ_3 and N, the overall shape does not. In the region labelled 'no axon' in figure 4, the steady-state solution of equations (6) is that the concentrations (and therefore the growth rates) all have equal values of $\tilde{C}_i = 1/N$. In this region all neurites continue to grow at equal rates with approximately equal lengths. In the 'axon formation' region a single neurite develops a concentration near 1 whereas all other neurites have small concentrations. The position of the instability curve was defined to be where the largest concentration reaches a value halfway between $\tilde{C}_i = 1/N$ and $\tilde{C}_i = 1$. The exact value defined for the transition is relatively unimportant because the transition between the two regions is rapid.

The shape of the instability curve contains information about the instability. There is a broad minimum extending across three orders of magnitude in χ_1; thus, aside from extreme low and high values, the instability is rather insensitive to the value of χ_1. In contrast, the dependence of the stability curve on χ_2 is quite sharp, with a transition to axon formation at approximately $\chi_2 = 10$ to 20. Remembering the definitions $\chi_1 = DAG/SV_{soma}$ and $\chi_2 = FS/\alpha G^2$ it is evident that because $\chi_1 = 0$ is always in the stable (no axon) region then diffusion must be present for instability to occur. Similarly, because $\chi_2 = 0$ is also always in the stable region anterograde transport must also be present ($F > 0$) for the instability to arise.

We have modelled the source term S as a constant, but it is reasonable that in a real neuron this parameter could change as cell development progresses. From the instability curve we can understand how changes in S will affect the development of the instability. If S decreases then χ_1 increases and χ_2 decreases. These changes in parameters could shift an axon-bearing cell across the instability line into the region of stability, perhaps corresponding to developmental stage 4, dendritic differentiation and growth.

Because we cannot calculate the values of χ_1 and χ_2 for a real neuron without knowing the identity of the determinant chemical, we used the shape of the instability curve to choose values of these parameters for our simulations. We chose $\chi_1 = 1$ so that we would be within that broad minimum of the instability curve and $\chi_2 = 100$ so that we would be within the axon-formation region and well away from the instability curve. The simulations presented in this paper were all done with the parameters $\chi_1 = 1$, $\chi_2 = 100$, $\chi_3 = 10$, and $N = 4$. None of the results that we present are dependent on these exact values: the results are qualitatively unchanged as long as the parameters do not approach the instability curve.

5. AXOTOMY EXPERIMENTS AND SIMULATIONS

The underlying assumptions of our simulation, that all neurites are initially equally competent and that a length-related instability determines the identity of the axon, are derived from the axotomy experiments of Dotti & Banker (1987) and Goslin & Banker (1989). For this model to be considered successful we should be able to reproduce the qualitative behaviour seen in these experiments.

We simulate axotomy by reducing the length of the axon at an arbitrary time ($\tilde{t} = 2$) after the identity of the axon has been established (see figure 2). Because C_i represents the concentration at the tip of the neurite (where growth is occurring) we must also alter that value to simulate an axotomy. As a simplification we assume that the concentration profile of the available determinant chemical is linear from the soma to the neurite tip; we calculate the new concentration from this profile and the new length of the cut neurite. Other models for the concentration profile may be used, but we have seen that the development of the simulation after an axotomy is only dependent on the chosen concentration profile if the axotomy leaves the original axon at a length close to that of the longest of the other neurites.

Figure 5 (*a*,*b*) shows two examples of axotomy simulations. In figure 5 (*a*) the axon is cut to a length that is still longer than (though comparable to) the length of the longest of the other neurites. The original axon quickly regains its rapid rate of growth and reforms the axon. In figure 5 (*b*) the original axon is cut to a length shorter than the other three neurites. In this case the longest neurite begins to grow rapidly and forms a new axon, while the original axon regrows only slightly to a length comparable to that of the other short neurites. Immediately after the axotomy, all the neurites experience a spurt of growth before a new axon emerges, in agreement with experiments (Goslin & Banker 1989) in which the axon was cut to a length comparable to that of the other neurites.

The differences in neurite length seem to play a more important role in these axotomy simulations than do the differences in determinant chemical concentration. In the simulation shown in figure 5 (*b*), the concentration at the new tip of the cut axon was still the largest by a factor of four. This concentration rapidly dropped, however, and it was the longest of the remaining neurites that became the new axon. This dominance of length difference in the axotomy simulations is consistent with the previously discussed dominance of length difference during initial axon formation.

Goslin & Banker (1989) observed that the latency for resumption of growth of an axon after axotomy was a function of the length difference between the two longest neurites, with a smaller length difference requiring a longer latency. The latency in our simulations shows the same qualitative behaviour (figure 6). At $\tilde{t} = 2$, when the simulation variables were close to a steady-state solution, we cut the axon to a random length and measured the time from axotomy

PHILOSOPHICAL TRANSACTIONS OF THE ROYAL SOCIETY B BIOLOGICAL SCIENCES

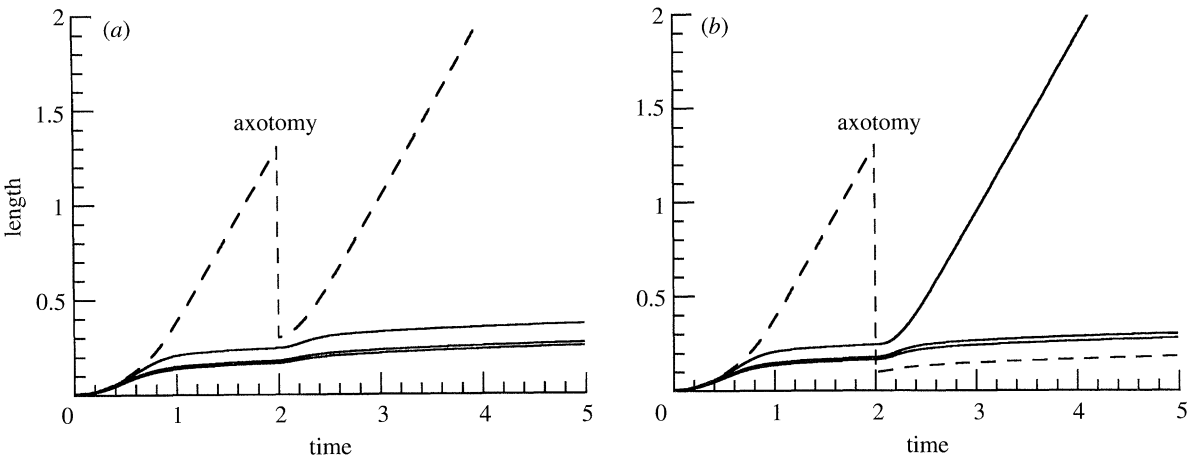

Figure 5. Axotomy of the growing axon. The dashed line represents the original axon. (*a*) The axon is cut to a length of 0.3, still longer than all the other neurites. The original axon reforms. (*b*) The axon is cut to a length of 0.1, shorter than the other neurites. The longest remaining neurite forms a new axon.

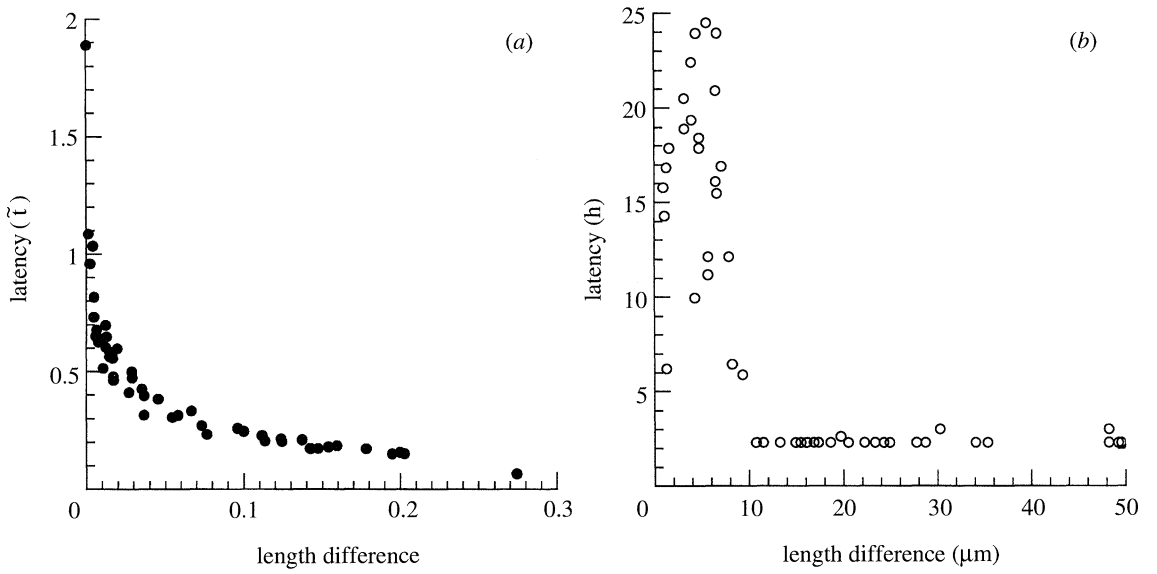

Figure 6. Latency of axon regeneration after axotomy plotted against the length difference between the two longest remaining neurites. (*a*) Data from the simulation. (*b*) Latency data from the axotomy experiments of Goslin & Banker (1989). Note that because the cells were not observed continuously the minimum latency time measurable in those experiments was 2 h.

to the beginning of rapid growth of a new axon, where rapid growth was arbitrarily defined as a growth rate halfway between the equal growth rate of $1/N$ and the maximum sustainable growth rate of 1.

6. RESPONSE TO SPATIAL VARIATIONS

Our model implicitly assumes that the outgrowth occurs in an isotropic and homogeneous environment. Although this may be attainable *in vitro* it is seldom the case for growth *in vivo*. We can remove the assumption of isotropic and homogeneous growth by allowing parameters to vary among the neurites.

The most straightforward parameter to vary is the growth parameter α. Changes in α for a given neurite directly change the growth rate of that neurite (see equation (4)). This may correspond to the effect of different growth substrates, or of a growth-stimulating chemical signal, such as nerve growth factor (Letourneau 1975; Gunderson & Barret 1980) or cyclic AMP (Zheng *et al.* 1994). We modelled this by varying α on neurite 1 while keeping α constant for all other neurites, for a series of 1000 simulations. The probability that neurite 1 formed the axon is plotted as a function of its change in α in figure 7. At $\Delta\alpha = 0$ all of the neurites had an equal probability of forming the axon (25% for 4 neurites). As α was increased the probability of axon formation by that neurite also increased and this probability reached 100% for $\Delta\alpha = +8\%$. Conversely, a negative $\Delta\alpha$ rapidly suppresses axon formation by that neurite.

This is a very sensitive dependence of axon formation on a small (10%) variation in α. One must remember that in these calculations the perturbation in α was

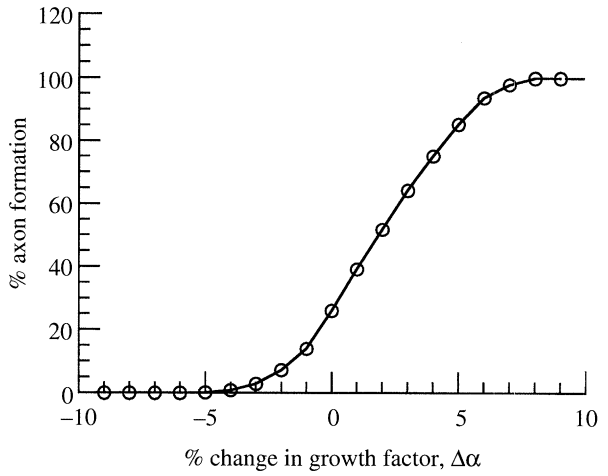

Figure 7. Dependence of axon-formation probability on a change in the growth factor α of one neurite only. The enhancement of growth in a particular neurite increases the probability of axon formation by that neurite. See the text for a detailed discussion.

made from the very beginning of the simulation. In reality perturbations in α are likely to occur later in neurite development, and it is reasonable that correspondingly larger perturbations would then be necessary to alter axon formation significantly. The conclusion that should be drawn from this calculation is that although the choice of the neurite that forms the axon is random under homogeneous environmental conditions this choice may easily become *deterministic* in an inhomogeneous environment. Axon formation by neurites in different locations may be inhibited or encouraged by their environment.

7. DISCUSSION: MECHANISMS, OTHER TESTS AND PREDICTIONS

Several mechanisms have previously been suggested to account for axon differentiation. One general possibility is that pre-existing internal cellular asymmetries bias one neurite to become the axon. Dotti & Banker (1991), however, found no evidence of correlations between site of axon initiation and asymmetry or position of the nucleus, Golgi complex or microtubule-organizing centre. Certain molecules, such as the membrane-associated phosphoprotein GAP-43 (also known as B-50, F1 or P-57) (Meiri *et al.* 1988; Goslin *et al.* 1988) and the microtubule-associated τ phosphoproteins (Binder *et al.* 1984; Tytell *et al.* 1984), are segregated to the axon soon after the axon can first be identified on morphological grounds; it has been suggested on this basis that these molecules could determine the axon. Although such segregated molecules may participate in the formation, stabilization or specialized function of the axon, the mechanism responsible for their segregation – and thus for the uniqueness of the axon – remains unknown. Thus such 'prepattern' hypotheses do not provide a full account of neuronal polarization. Moreover, prepattern mechanisms are inconsistent with the observed outcome of axotomy experiments, as described above.

To avoid these difficulties, Kosik & Caceres (1991) hypothesized that a phosphatase-mediated cooperative dephosphorylation of microtubule-associated proteins such as τ, acting stochastically within each neurite to increase microtubule stability and consequent elongation, could account for the emergence of a fastest-growing neurite as the axon; evidence for a distally increasing gradient in the ratio of dephosphorylated to phosphorylated τ has recently been obtained (Rebhan *et al.* 1995). Such a mechanism may indeed participate in axon differentiation, but cannot, by itself, account for the inhibition of other neurites' growth. Kosik & Caceres thus found it necessary to posit the existence of 'some feedback inactivation from the elongating neurite, perhaps the putative phosphatase' itself.

The model presented here does not require such specific inactivating factors. Instead, our model proposes that polarization results from competition for a diffusible, anterograde-transportable 'determinant chemical', produced in the soma, whose concentration at the neurite tip affects the rate of outgrowth. Similar competition among neurites for some material has often been invoked to explain synapse elimination and other 'pruning' effects on axonal arborization (Devor & Schneider 1975; Van Essen 1982; Smalheiser & Crain 1984). If, however, the rate of anterograde transport increases with rate of outgrowth, this competition for an endogenous determinant chemical will lead to a positive-feedback, winner-take-all instability in which a single neurite – the axon – grows rapidly and all other neurites slow.

Diffusion of transported determinant chemical back from the neurite tips opposes the positive feedback and is responsible for the slowing of growth in 'losing' neurites as their tips come to equilibrium with the soma. The rate of anterograde transport could be coupled to growth rate by at least two mechanisms. The growing tip exerts tension on the neurite (Lamoureux *et al.* 1989), and increased growth may lead hydrostatically to increased flow of cytosol into the proximal neurite. If the anterograde transport mechanism is not saturated, then this increased proximal inflow will allow increased loading, and thus transport, of the determinant chemical. Alternatively, capacity or velocity of the transport mechanism could be increased by the growth-associated increase in neurite tension if the increased strain energy leads to conformational changes (Heidemann & Buxbaum 1994) in transport proteins.

If our model is to be more than a heuristic device, it must be amenable to experimental test. Possible tests of the model are suggested by inspection of equations (1–4): manipulation of the terms in those equations should in principle yield experimentally testable predictions. It is difficult to imagine methods for the selective modification of D, A, V_{soma} or V_{tip} that would not introduce complicating extraneous effects, but some of the other terms should be more tractable. Because the net transfer rate T_i is central to our model, analysis and manipulation of terms in equation (2) should be particularly revealing. The model was based largely upon the axotomy observations of Dotti & Banker (1987) and Goslin & Banker (1989); axotomy

PHILOSOPHICAL TRANSACTIONS OF THE ROYAL SOCIETY B BIOLOGICAL SCIENCES

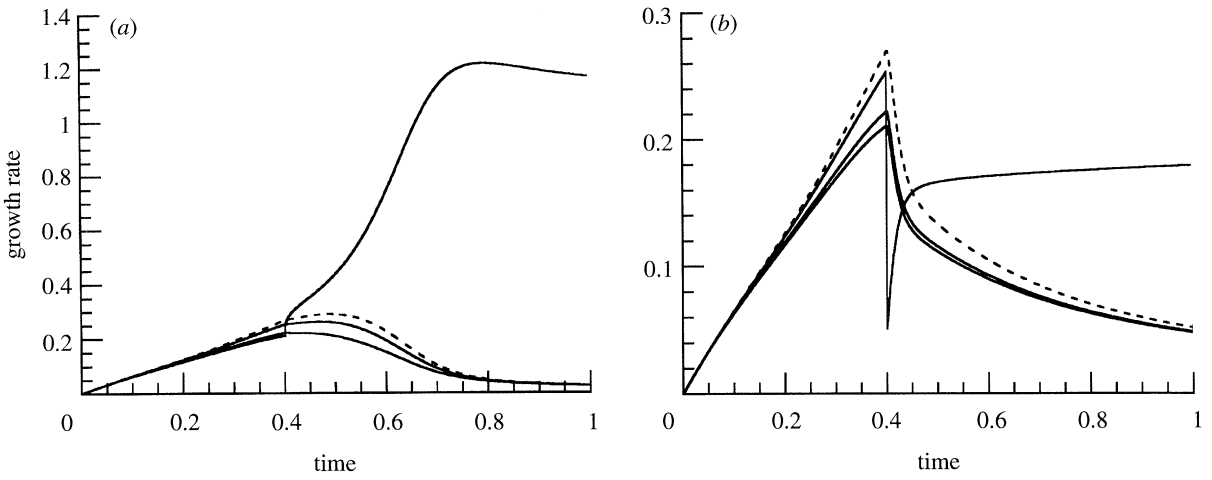

Figure 8. (*a*) Effect of increased growth rate on axon differentiation. The growth rate of the shortest neurite was increased by 20% at $\tilde{l} = 0.4$. This neurite now forms the axon; the other neurites, including the previously fastest growing (denoted by the dashed line), are inhibited. This result corresponds to the experimentally observed behaviour in cells where outgrowth of a single neurite is enhanced by focal application of cAMP (Zheng *et al.* 1994). (*b*) Effect of decreasing one neurite's growth rate while increasing its rate of anterograde transport. The growth of all the neurites is inhibited. This result corresponds to the experimentally observed behaviour in cells where a single neurite is perfused with cAMP and colchicine (Zheng *et al.* 1994).

in our model is represented by reductions in L_i and C_i – both of which contribute to T_i – and, as noted above, the outcome of such simulated axotomy is in qualitative agreement with the experimental observations.

More recently, Zheng *et al.* (1994) conducted a series of experiments studying the effects of focal perfusion of individual growth cones on the rates of outgrowth of the perfused and non-perfused neurites. Perfusion with 8-br-cAMP increased the growth rate of the perfused neurite and inhibited the growth of the remaining neurites; expressing the growth-enhancing effect of cAMP as an increase in α for the perfused neurite, and thus in $(\mathrm{d}L_i/\mathrm{d}t)$ (equation (4)), our model yields similar results (figure 8*a*). More difficult to interpret are the results of combined perfusion with 8-br-cAMP and colchicine. Perfusion with colchicine alone caused the perfused neurite to retract, with no significant effect on the other neurites; this is predicted by our model if the other neurites were growing, i.e. if the perfused neurite was not the axon. However, combined application of 8-br-cAMP and colchicine lowered the growth rate not only of the perfused neurite but of the non-perfused neurites as well. From this observation, Zheng *et al.* concluded that increased growth of the perfused neurite could not be the cause of slowing in the other neurites; they suggested that the slowing could be due to a cAMP-mediated increase in transport within the perfused neurite (Azhderian *et al.* 1994). In our model, inhibition of growth in the 'losing' neurites results not from increased axonal growth *per se* but from increased net transfer – which may be due to increased growth or to effects of modulating factors – of the determinant chemical from the soma to the growing axon, leaving less for the growth of the other neurites. Thus, in our model, increasing anterograde transport while reducing growth in a single neurite (by increasing F, or alternatively I_i, and decreasing α in that neurite) inhibits outgrowth in all other neurites (figure 8*b*), in qualitative agreement with the observations of Zheng *et al.*

Other tests involving T_i can be proposed. The rate of neurite outgrowth, $\mathrm{d}L_i/\mathrm{d}t$, can be reduced by culture in medium with a low calcium concentration (Campenot & Draker 1989). Under such conditions, growth of a single neurite might be increased by focal perfusion with medium of normal calcium concentration, without cAMP's complicating effects on anterograde transport. Our model predicts that such a neurite, even if initially not the longest, will become the axon, but that (assuming calcium has no effect on net transfer) combined perfusion with normal calcium and colchicine will not inhibit growth of the other neurites. The rate of neurite outgrowth can also be increased mechanically, by experimentally applied mechanical tension (Bray 1984; Heidemann & Buxbaum 1994); our model predicts that by such 'towing' an initially short and slow-growing neurite could be made to become the axon.

Our model assumes that T_i increases with neurite growth rate; a crucial test would therefore be the direct measurement of T_i in growing neurites. This, and tests involving S or C_i, is not possible without knowing the identity of the determinant chemical. As previously mentioned, there are indications that τ, or particularly dephospho-τ, may be the determinant chemical: by stabilizing microtubule polymerization in the presence of excess tubulin, τ could exert the requisite concentration-dependent control of growth rate at the neurite tip. Suppression of neuronal τ production by means of antisense oligonucleotides can prevent axon formation without inhibiting neurite production (Caceres & Kosik 1990; Caceres *et al.* 1991); and baculovirus-mediated expression of high concentrations of τ in normally round non-neuronal cells can induce the

PHILOSOPHICAL TRANSACTIONS OF THE ROYAL SOCIETY B BIOLOGICAL SCIENCES

formation of single long axon-like processes with plus-end distal microtubules (Knops *et al.* 1991). This effect is not obtained with other MAPs: high-level expression of MAP2C in the same non-neural cells leads to multiple shorter processes (LeClerc *et al.* 1993). If τ is the determinant chemical, these manipulations can be interpreted in terms of the stability map (figure 4) and equation (7*b*): decreasing S shifts a normally axon-forming neuron below the instability curve into the 'no axon' region, whereas increasing S shifts a normally rounded cell into the region of axon formation.

After axotomy, in a small fraction of cases the new axon is formed by a neurite that is shorter than the axonal stump (Goslin & Banker 1989). Our model predicts that a shorter neurite will form the new axon if its net transfer rate of the determinant chemical is, at the time of axotomy, greater than that of the axonal stump. To test this prediction, developing neurons could be injected with a fluorescent-labelled anterograde-transportable marker (e.g. fluorescein-τ) shortly before axotomy, and the rate of fluorescence accumulation in the neurites compared. Similarly, the model predicts that, with a sufficiently sensitive marker, the presumptive axon could be identified as the neurite with the greatest net transfer rate, even before its manifestation of rapid growth. These methods would also allow a test of the predicted coupling between transfer and growth rates, by 'towing' a neurite of a marker-injected cell.

The model presented here does not specifically address such important aspects of neuronal polarization as the segregation of ribosomes, certain proteins such as MAP2, and other cellular elements to the somatodendritic compartment, or the differential orientation of microtubules (exclusively plus-end distal in the axon; both plus-end and minus-end distal in dendrites). These phenomena, however, are not incompatible with our model. Substances that can be conveyed by the anterograde transport mechanism would tend to segregate to the axon; proteins competing with such segregated substances for cytoskeletal binding could thereby be excluded from the axon. As noted above, τ proteins segregate to the axon, and it has been suggested that they displace MAP2 from axonal binding sites (Schoenfeld & Obar 1994), although available biochemical evidence concerning such competitive binding is inconclusive (Kim *et al.* 1986). In addition, if substances that selectively cap minus ends, preventing their elongation, segregate to the axon, axons would contain only (the faster-growing) plus-end-distal microtubules; in dendrites, in the absence of such selective caps, the initial preponderance of the faster-growing plus-end-distal microtubules would in time equilibrate with slower-growing minus-end-distal microtubules so that both orientations occurred. Cellular elements would thus be transported from the soma along minus-end distal microtubules (as is the case for ribosomes (Stebbings & Hunt 1983)) into the dendrites, but would be excluded from the axon, if they selectively bound dynein (responsible for transport toward the minus-end) rather than kinesin (responsible for transport toward the plus-end).

The authors thank Dr Gary Banker and an anonymous referee for their valuable comments. This work was supported by grants from the U.S. National Science Foundation (IBN-9221654), the Canadian Natural Sciences and Engineering Research Council, and the Sandoz Foundation for Gerontological Research.

REFERENCES

Azhderian, E. M., Hefner, D., Lin, C. H., Kaczmarek, L. K. & Forscher, P. 1994 Cyclic AMP modulates fast axonal transport in Aplysia bag cell neurons by increasing the probability of single organelle movement. *Neuron* **12**, 1223–1233.

Binder, L. I., Frankfurter, A. & Rebhun, L. I. 1984 The distribution of tau in the mammalian central nervous system. *J. Cell Biol.* **101**, 1371–1378.

Brady, S. T. 1991 Molecular motors in the nervous system. *Neuron* **7**, 521–523.

Bramburg, J. R., Bray, D. & Chapman, K. 1986 Assembly of microtubules at the tip of growing axons. *Nature, Lond.* **321**, 788–790.

Bray, D. 1984 Axonal growth in response to experimentally applied mechanical tension. *Devl Biol.* **102**, 379–389.

Caceres, A. & Kosik, K. S. 1990 Inhibition of neurite polarity by tau antisense oligonucleotides in primary cerebellar neurons. *Nature, Lond.* **343**, 461–463.

Caceres, A., Potrebic, S. & Kosik, K. S. 1991 The effect of tau antisense oligonucleotides on neurite formation of cultured cerebellar macroneurons. *J. Neurosci.* **11**, 1515–1523.

Campenot, R. B. & Draker, D. D. 1989 Growth of sympathetic nerve fibers in culture does not require extracellular calcium. *Neuron* **3**, 733–743.

Cheney, E. W. & Kincaid, D. R. 1980 *Numerical mathematics and computing*. Monterey, California: Brooks/Cole.

Craig, A. M. & Banker, G. A. 1994 Neuronal polarity. *A. Rev. Neurosci.* **17**, 267–310.

Craig, A. M., Wyborski, R. J. & Banker, G .A. 1995 Preferential addition of newly synthesized membrane protein at axonal growth cones. *Nature, Lond.* **375**, 592–594.

Devor, M. & Schneider, G. 1975 Neuroanatomical plasticity: The principle of conservation of total axonal arborization. In *Aspects of neural plasticity* (INSERM Colloquia, Vol. 43), ed. F. Vital-Durand & M. Jeannerod, pp. 191–200. Paris: Editions d'INSERM.

Dotti, C. G. & Banker, G. A. 1987 Experimentally induced alterations in the polarity of developing neurons. *Nature, Lond.* **330**, 254–256.

Dotti, C. G. & Banker, G. A. 1991 Intracellular organization of hippocampal neurons during the development of neuronal polarity. *J. Cell Sci.* (Suppl.) **15**, 75–84.

Dotti, C. G., Sullivan, C. A. & Banker, G. A. 1988 The establishment of polarity by hippocampal neurons in culture. *J. Neurosci.* **8**, 1454–1468.

Goslin, K. & Banker, G. A. 1989 Experimental observations on the development of polarity by hippocampal neurons in culture. *J. Cell Biol.* **108**, 1507–1516.

Gordon-Weeks, P. R. 1991 Control of microtubule assembly in growth cones. *J. Cell Sci.* (Suppl.) **15**, 45–49.

Goslin, K., Schreyer D. J., Skene, J. H. P. & Banker, G. A. 1988 Development of neuronal polarity: GAP-43 distinguishes axonal from dendritic growth cones. *Nature, Lond.* **336**, 672–674.

Gunderson, R. W. & Barret, J. N. 1980 Characterization of the turning response of dorsal root neurites toward nerve growth factor. *J. Cell Biol.* **87**, 546–554.

PHILOSOPHICAL TRANSACTIONS OF THE ROYAL SOCIETY B BIOLOGICAL SCIENCES

Heidemann, S. R. & Buxbaum, R. E. 1994 Mechanical tension as a regulator of axonal development. *Neurotoxicology* **15**, 95–108.

Kim, H., Jensen, C. G. & Rebhun, L. I. 1986 The binding of MAP-2 and tau on brain microtubules *in vitro*: Implications for microtubule structure. *Ann. N.Y. Acad. Sci.* **466**, 218–239.

Knops, J., Kosik, K. S., Lee, G., Pardee, J. D., Cohen-Gould, L. & McConlogue, L. 1991 Overexpression of tau in a nonneuronal cell induces long cellular processes. *J. Cell Biol.* **114**, 725–733.

Kosik, K. S. & Caceres, A. 1991 Tau protein and the establishment of an axonal morphology. *J. Cell Sci.* (Suppl.) **15**, 69–74.

Lamoureux, P., Buxbaum, R. E. & Heidemann, S. R. 1989 Direct evidence that growth cones pull. *Nature, Lond.* **340**, 159–162.

LeClerc, N., Kosik, K. S., Cowan, N., Pienkowski, T. P. & Bass, P. W. 1993 Process formation in Sf9 cells induced by the expression of a microtubule-associated protein 2C-like construct. *Proc. natn. Acad. Sci. U.S.A.* **90**, 6223–227.

Letourneau, P. C. 1975 Possible roles for cell-to-substratum adhesion in neuronal morphogenesis. *Devl Biol.* **44**, 77–91.

Letourneau, P. C. & Ressler, A. H. 1984 Inhibition of neurite initiation and growth by taxol. *J. Cell Biol.* **98**, 1355–1362.

Mansfield, S. G., Diaz-Nido, J., Gordon-Weeks, P. R. & Avila, J. 1991 The distribution and phosphorylation of the microtubule-associated protien MAP 1B in growth cones. *J. Neurocytol.* **20**, 1007–1022.

Matus, A 1988 Microtubule-associated proteins: their potential role in determining neuronal morphology. *A. Rev. Neurosci.* **11**, 29–44.

Meiri, K. F., Willard, M. & Johnson, M. I. 1988 Distribution and phosphorylation of the growth-associated protein GAP-43 in regenerating sympathetic neurons in culture. *J. Neurosci.* **8**, 2571–2581.

Rebhan, M., Vacun, G. & Rosner, H. 1995 Complementary distribution of tau proteins in different phosphorylation states within growing axons. *NeuroReport* **6**, 429–432.

Schoenfeld, T. A. & Obar, R. A. 1994 Diverse distribution and function of fibrous microtubule-associated proteins in the nervous system. *Int. Rev. Cytol.* **151**, 67–137.

Skene, J. H. P. 1989 Axonal growth associated proteins. *A. Rev. Neurosci.* **12**, 127–156.

Smalheiser, N. R. & Crain, S. M. 1984 The possible role of 'sibling neurite bias' in the coordination of neurite extension, branching, and survival. *J. Neurobiol.* **15**, 517–529.

Stebbings, H. & Hunt, C. 1983 Microtubule polarity in the nutritive tubes of insect ovarioles. *J. Cell Sci.* **6**, 133–141.

Tytell, M., Brady, S. T. & Lasek, R. J. 1984 Axonal transport of a subclass of tau proteins: Evidence for the regional differentiation of microtubules in neurons. *Proc. natn. Acad. Sci. U.S.A.* **81**, 1570–1574.

Van Essen, D. 1982 Neuromuscular synapse elimination. In *Neuronal development*, ed. N. Spitzer, pp. 333–376. New York: Plenum Press.

Zheng, J. Q., Zheng, Z. & Poo, M. 1994 Long-range signaling in growing neurons after local elevation of cyclic AMP-dependent activity. *J. Cell Biol.* **127**, 1693–1701.

(*Received 23 October 1995; accepted 26 February 1995*)

PHILOSOPHICAL TRANSACTIONS OF THE ROYAL SOCIETY B BIOLOGICAL SCIENCES